Acta Cryst. (1997). A**53**, 493–504

A Universal Treatment of X-ray and Neutron Diffraction in Crystals. II. Extinction†

HUA-CHEN HU

China Institute of Atomic Energy, Graduate School of Nuclear Industry, PO Box 275(18), Beijing 102413, People's Republic of China. E-mail: ciaednp@sun.ihep.ac.cn

(*Received 19 May 1995; accepted 13 March 1997*)

Abstract

Based on the formalism for calculating the integrated reflection power ratio of a plane mosaic crystal by using three dimensionless parameters as described in paper I [Hu (1997). *Acta Cryst.* A**53**, 000–000], exact and universal expressions for the secondary-extinction factors in X-ray and neutron crystallography are developed that can be applied to reflections of all possible values of extinction factor, reflection symmetry and the absorption-to-scattering cross-section ratio of the crystal. The representation by three parameters gives a clear and definite physical meaning to the concept of extinction. The theory has been extended to treat the extinction of a spherical crystal, and the striking difference in the evaluated secondary-extinction factor between the equivalent single-plate and the exact method in the spherical-crystal treatment under $\theta_B = 0°$ is explained. As a demonstration of the feasibility of using these expressions, the diffraction data for LiF and MgO crystal plates measured by Lawrence [*Acta Cryst.* (1972), A**28**, 400–404; (1973), A**29**, 208–210] are reanalyzed by this method. All the reflections including the strongest ones (Y_o down to 0.026) are reanalyzed simultaneously with single-valued particle size and mosaic spread as fitting parameters and allowing for primary extinction if necessary. The results (R factor = 0.014 and 0.053 for LiF and MgO, respectively) are unprecedentedly good. Furthermore, in disagreement with Lawrence, the extinction of LiF is found to be of secondary type and in the case of MgO both primary and secondary extinction should be considered. The analysis also shows that the formula $Y \sim Y_p Y_s$ is valid only for very weak extinctions and that the Hamilton–Darwin equations are valid in a range much broader than previously anticipated.

1. Introduction

The treatment of extinction in X-ray and neutron crystallography is a fundamental topic in diffraction theory and has long been an important problem in structure-factor refinement. Extinction was first proposed by Darwin (1914) and described in terms of his mosaic model (Darwin, 1922). Hamilton (1957, 1963) first studied the dependence of extinction on crystal shape. Zachariasen (1967) gave a general theoretical treatment for extinction in the X-ray case, Becker & Coppens (1974) significantly improved Zachariasen's theory and thereafter their methods have been widely used in structure-factor refinement in the limit of small extinction (less than 20%). For further investigation of this problem, Borie (1982) mentioned the importance of the absorption-to-scattering cross-section ratio. Werner (1974) gave a solution of the Hamilton–Darwin transfer equations to express the extinction factor for a parallelepiped crystal and analyzed the contributions to the extinction factor for neutrons reflected one, three and five times. One may list other papers related to this problem such as the treating of the inhomogeneity in the mosaic structure (Schneider, 1977), the treatment of extinction for a mosaic crystal plate (Mazzone, 1981; Suortti, 1982; Yelon, van Laar, Kaprzyk & Maniawski, 1984; Yelon, van Laar, Maniawski & Kaprzyk, 1984; Palmer & Jauch, 1995) and the numerical approximation for the imperfect crystal (Wilkins, 1981). Kato (1976, 1980) investigated the secondary extinction and the combination of both primary and secondary extinction with statistical dynamical theory. Sabine reconciliated different extinction theories (Sabine, 1988) and derived the extinction factor for a cubic shaped crystal (Sabine, 1995; Kampermann, Sabine & Craven, 1995). Whatever achievements have been made by these authors, however, the problem of treatment of severe extinction remains unresolved. To deal with this situation, experimentalists have used very thin (as thin as 10 μm) crystals in their measurements in order to avoid the difficulties in determining the extinction factor due to strong reflections in thick crystals.

In this paper, the secondary extinction for diffraction from mosaic crystal plates is treated through exact solutions for the integrated reflection power ratio (here referred to as IRPR) expressions using three dimensionless parameters as described in the preceding paper (Hu, 1997; hereafter referred to as I). In §2.1, the two universal exact expressions for the secondary extinction in the case of plane-crystal geometry will be described in detail, as well as their behavior and their relation to the three dimensionless parameters: an asymmetry factor b, the ratio ξ of the absorption to the scattering

† Project supported by National Natural Science Foundation of China and Science Foundation of Nuclear Industry of China.

cross section and the reduced thickness A_k of the crystal. §2.2 is an extension of this theory to the case of a spherical crystal. In §3, two experimental studies of the X-ray diffraction for crystal plates carried out by Lawrence (1972, 1973*a*,*b*; hereafter referred to as *L*1972, *L*1973*a*,*b*) on LiF and MgO, a long-standing test case in the analysis of diffraction data, are analyzed by our method as examples of its practical application and as a demonstration of the usefulness of the new extinction formalism.

2. Extinction

If there is no primary extinction, the term 'secondary extinction' may be considered as referring to the ratio between the integrated reflection power ratio (IRPR) resulting from multiple reflection and absorption within the crystal and the IRPR due to a single reflection based on the kinematic approximation without extinction. Secondary extinction for a plane and a spherical crystal according this definition is treated as follows.

2.1. *Plane crystal*

Just as in I, the mosaic distribution of the crystal is assumed to be Gaussian, and the diffraction geometry to be as depicted in Fig. 1 of I. Like the expressions for the IRPR of a plane crystal that appeared in I, all expressions for the secondary-extinction factor may be used here for any incident-beam width.

Single reflection for a plane mosaic crystal can in practice be considered to occur in two cases:

(*a*) For a thin crystal when the condition $R_H^\theta = Qt_0/\cos\theta_o$ is met. This is depicted in Fig. 6 of I as the straight line from the origin. For example, in Fig. 6(*a*), when $\xi_0 = 0.1$ and $|b| = 1$, this condition is satisfied only for $A_{k0} < 0.1$. The physical meaning of this result is that the path length traveled by the neutron (or X-ray) should be much less than one scattering mean free path so that most of the reflected beams suffer only one reflection.

(*b*) For absorbing crystals, no matter the thickness, when $\xi_0 > 10$. This is depicted in Fig. 7 of I. The physical meaning is that the absorption mean free path of the sample is much smaller than the scattering mean free path, and so nearly all the exit beam comes from a single reflection. The IRPR can be expressed by (30), (32) and (33) of I for Bragg and Laue cases, respectively. This is the normal case in X-ray crystallography for most of the crystals with atomic number $Z > 20$ and $\eta > 2'$ and is valid also for strongly absorbing crystals in the neutron case.

For all cases other than (*a*) and (*b*), the effect of multiple reflections may not be neglected and hence secondary-extinction effects must be considered. Because single reflection can effectively occur for cases both (*a*) without absorption and (*b*) with absorption, as described above, the definition of secondary extinction can accordingly be expressed in two different forms, (*a*) Y_ν and (*b*) Y_μ. The IRPR both for single reflection and for multiple reflection can be expressed in terms of the three dimensionles parameters Σ_{s0}, ξ_0 and A_{k0}. Thus, the Y_ν and Y_μ can also be expressed in terms of the same parameters through variable transformation as

$$Y_\nu = \frac{R_H^\theta}{Qt_0 \sec\theta_o} = \frac{R_H^\theta/\eta}{(2\pi)^{1/2}A_{k0}} \tag{1}$$

$$Y_\mu = \frac{R_H^\theta/\eta}{QA_c/\eta}. \tag{2}$$

From the definition of A_{k0} and ξ_0 as well as the IRPR for single reflection for the Bragg and Laue cases, *i.e.* (25)–(27), (30) and (32)–(33) in I, QA_c/η can be expressed as:
for the Bragg case:

$$QA_c/\eta = [(2\pi)^{1/2}/(1-b)\xi_0] \times \{1 - \exp[-(1-b)\xi_0 A_{k0}]\}; \tag{3}$$

for the Laue case ($b = 1$):

$$QA_c/\eta = (2\pi)^{1/2}A_{k0}\exp(-\xi_0 A_{k0}); \tag{4}$$

for the Laue case ($b \neq 1$):

$$QA_c/\eta = [(2\pi)^{1/2}/(1-b)\xi_0] \times [\exp(-b\xi_0 A_{k0}) - \exp(-\xi_0 A_{k0})]. \tag{5}$$

Note that the right sides of (3)–(5) will be $(2\pi)^{1/2}A_{k0}$ when ($\xi_0 = 0$), *i.e.* (2) and (1) are identical in this case.

When primary extinction occurs, $Y_p\Sigma_{s0}$ is used instead of Σ_{s0} (Werner, 1974). This causes all the parameters containing Σ_{s0} such as A_{k0}, ξ_0 that appear in (1) and (2) to contain Y_p implicitly through the modified Σ_{s0} factor. However, by definition, the denominators of (1) and (2) are the extinction-free kinematic approximation of the IRPR, so here it should be divided by Y_p to restore its physical meaning when we use the three-parameter representation for treating data with extinction.

The relationship of the secondary-extinction factor to the three dimensionless parameters can be derived directly from the relationship of R_H^θ to these parameters as depicted in Figs. 6 and 7 of I.

Fig. 1 illustrates the dependence of the secondary extinction Y_ν upon A_{k0} for symmetric geometry. One can see clearly the remarkable reduction of Y_ν with increasing ξ_0 and A_{k0}. For the asymmetric case, such a dependence can be obtained through the ratio of R_H^θ to $Qt\sec\theta_0$ in Fig. 6(*b*) in I and one can anticipate a remarkable decrease of Y_ν with increasing b for a given ξ_0.

Fig. 2 depicts the dependence of Y_μ on A_{k0} for different ξ_0 under symmetric geometry. For the Laue

case, all the curves of Y_μ *versus* A_{k0} for different ξ_0 degenerate into a single curve identical to the Y_ν curve for the symmetric Laue case for $\xi_0 = 0$, as depicted in Fig. 1. This is because, in the latter case, the absorption and scattering can be treated separately in the expression for the IRPR. Fig. 2 also shows that Y_μ becomes linear and insensitive to ξ_0 only for very small A_{k0} for the Bragg case. However, these curves disperse when A_{k0} increases. We note that, for example, the value of Y_μ for $\xi_0 = 1.5$ goes down to its plateau around $A_{k0} \geq 1$, which is nearly the same A_{k0} position when the IRPR reaches its saturation value in Fig. 6(*a*) in I. This A_{k0} value, in fact, represents the depth of penetration of the incident beam in the crystal.

Figs. 3(*a*) and (*b*) depict the dependence of Y_μ on A_{k0} for different b in the case of $\xi_0 = 0.1$ and 2.0, respectively. Fig. 3(*b*) shows a very pronounced dependence of Y_μ on b for the Laue case. For the Bragg case, the range of A_{k0}, which is sensitive to b and shrinks when ξ_0 rises, finally becomes insensitive to b.

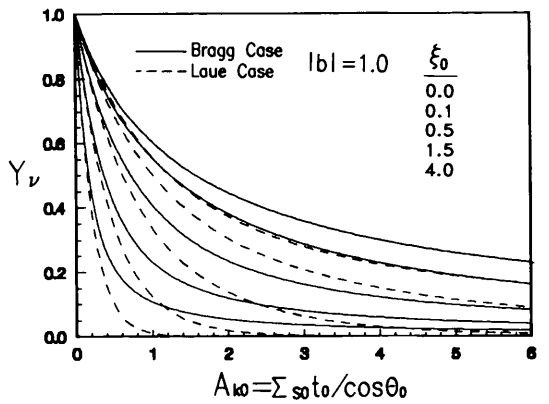

Fig. 1. The secondary-extinction factor Y_ν for a plane mosaic crystal as a function of reduced thickness A_{k0} for $|b| = 1$ and for different values of ξ_0.

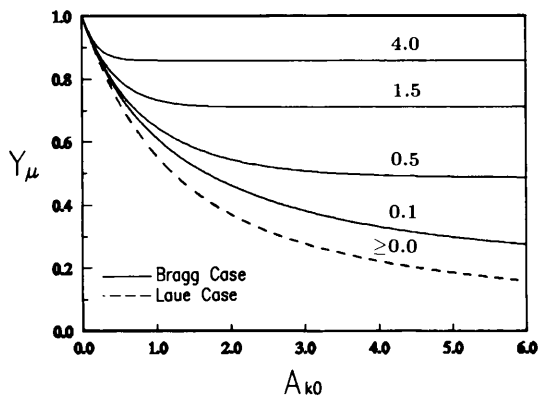

Fig. 2. The secondary-extinction factor Y_μ for a plane mosaic crystal as a function of reduced thickness A_{k0} for $|b| = 1$ and different values of ξ_0.

Fig. 4 depicts the dependence of Y_μ on ξ_0 for different b in the Bragg case. Y_μ is rather insensitive to b and gives the same curve for both b and $1/b$ (see Appendix A in I). The reciprocity relation is true for Y_ν when t_0, η and ξ_0 of the crystal are defined. Y_μ changes rapidly

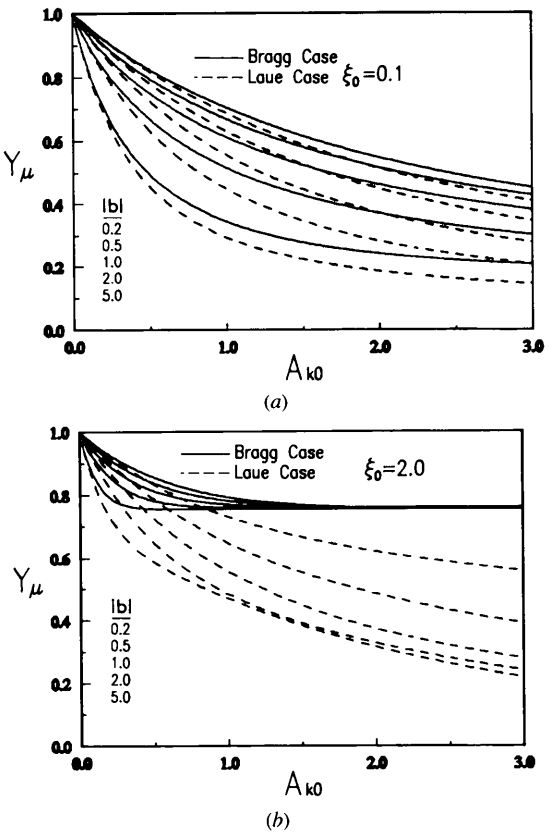

Fig. 3. The secondary-extinction factor Y_μ for a plane mosaic crystal as a function of ξ_0, reduced thickness A_{k0} and asymmetry parameter b.

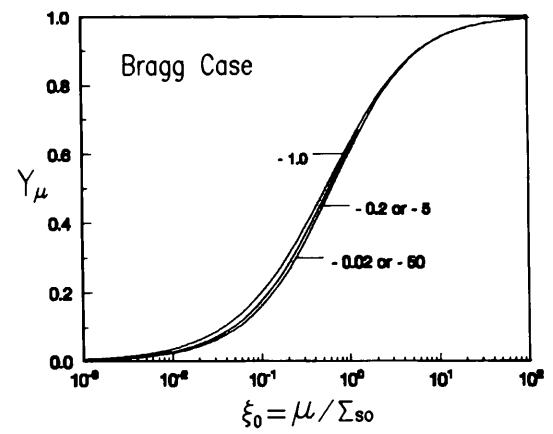

Fig. 4. The relationship between ξ_0 and the secondary-extinction factor Y_μ for a plane mosaic crystal of infinite thickness t_0; the parameters on the curves give values of b.

with ξ_0 and, unlike Y_ν, increases with increasing ξ_0 and approaches the saturation value unity when $\xi_0 > 10$. For example, $Y_\mu = 0.935$ when $\xi_0 = 10$, which means that the contribution of multiple reflections is only about 10% in the total IRPR.

2.2. *Spherical crystal*

When a spherical crystal of radius R is immersed in a homogeneous incident beam and the diffracted beam is collected by a detector recording the total reflecting power, we can express the secondary-extinction factor in two different forms, Y_ν and Y_μ, just as in the plane-crystal case mentioned before.

It is impossible to obtain an exact solution of the Hamilton–Darwin equations (hereafter referred to as H–D equations) for a spherical crystal except for the extreme cases $\theta_B = 0$ and $\pi/2$.

We may apply the formulae for the reflection power ratio for a crystal plate in the symmetric Laue and Bragg cases deduced from equations (2*a*) and (2*b*) of I to express the reflection power ratio for $\theta_B = 0$ and $\pi/2$, respectively. Thus,

for $\theta_B = \pi/2$, $\mu \neq 0$:

$$(P_H/P_0)(\xi, A_k) = \{1 - \exp[-2(\xi^2 + 2\xi)^{1/2} A_k]\} \times \{(\xi^2 + 2\xi)^{1/2} + \xi + 1 + [(\xi^2 + 2\xi)^{1/2} - (\xi + 1)] \times \exp[-2(\xi^2 + 2\xi)^{1/2} A_k]\}^{-1}; \quad (6)$$

for $\theta_B = \pi/2$, $\mu = 0$:

$$(P_H/P_0)(0, A_k) = A_k/(1 + A_k); \quad (7)$$

for $\theta_B = 0$ and all μ:

$$(P_H/P_0)(\xi, A_k) = \exp(-\xi A_k)[1 - \exp(-2A_k)]/2. \quad (8)$$

The IRPR for $\theta_B = \pi/2$ and 0 can be obtained by angular integration of (6)–(8).

In order to evaluate the angular dependence of the secondary-extinction factor of a spherical crystal, a proper expression of the angular dependence of IRPR for single and multiple reflection for a definite θ_B should first be formulated. As described by Becker & Coppens (1974) and Sabine (1988), this can only be approximately realized by interpolating from the values for 0 and $\pi/2$. Assume

$$(R_H^{\theta, \theta_B}/\eta)(\xi_0, \Sigma_{s0}R) \simeq (R_H^{\theta, 0}/\eta)(\xi_0, \Sigma_{s0}R)\cos^2\theta_B + (R_H^{\theta, \pi/2}/\eta)(\xi_0, \Sigma_{s0}R)\sin^2\theta_B \quad (9)$$

and

$$(QA_c^{\theta_B}/\eta)(\xi_0, \Sigma_{s0}R) \simeq (QA_c^0/\eta)(\xi_0, \Sigma_{s0}R)\cos^2\theta_B + (QA_c^{\pi/2}/\eta)(\xi_0, \Sigma_{s0}R)\sin^2\theta_B. \quad (10)$$

Sabine (1988) gave an approximate expression for the secondary-extinction factor of a cylindrical crystal with radius ρ for the non-absorbing case through the ratio of (9) to QV. His result for a given θ_B at $\Sigma_{s0}\rho = 5$ is smaller than the result based on numerical calculation of Hamilton (1963) with a maximum deviation of 10%. Also, the result of A_c calculated by (10) for a given θ_B at $\mu\rho \leq 5$ is smaller than the result listed in *International Tables for X-ray Crystallography* (1972) (*ITXCr*) with a maximun deviation of 12%. So it seems reasonable to use an approximate presentation of Y_μ through the ratio of (9) to (10).

There are three possible methods that may be used for approximate calculation of the IRPR for multiple and single reflection for a given θ_B.

(*a*) The diffraction geometry may be approximated by an incident beam of area πR^2 diffracted from a plate with a mean path length of $3R/2$. Hence, the IRPR for multiple and single reflection of a spherical crystal under $\theta_B = 0$ and $\pi/2$ can be obtained by substituting $3\Sigma_s R/2$ and $3\Sigma_{s0}R/2$ for A_k and A_{k0} in (6)–(8) and (3), (4), respectively, *i.e.*

$$\phi_1^{\theta_B}(\xi, 3\Sigma_{s0}R/2) = \pi R^2 (R_H^{\theta, \theta_B}/\eta)(\xi_0, 3\Sigma_{s0}R/2) \quad (11)$$

$$\psi_1^{\theta_B}(\xi, 3\Sigma_{s0}R/2) = \pi R^2 (QA_c^{\theta_B}/\eta)(\xi_0, 3\Sigma_{s0}R/2), \quad (12)$$

where $\phi_1^{\theta_B}$ and $\psi_1^{\theta_B}$ can then be approximated as in the right sides of (9) and (10), respectively. Thus, Y_ν and Y_μ can be expressed as

$$Y_\nu(\xi_0, \Sigma_{s0}R, \theta_B) = \frac{\phi_1^{\theta_B}(\xi_0, 3\Sigma_{s0}R/2)}{\pi R^2 3QR/2\eta} = \frac{2^{1/2}\phi_1^{\theta_B}(\xi_0, 3\Sigma_{s0}R/2)}{3\pi^{3/2}\Sigma_{s0}R^3} \quad (13)$$

$$Y_\mu(\xi_0, \Sigma_{s0}R, \theta_B) = \frac{\phi_1^{\theta_B}(\xi_0, 3\Sigma_{s0}R/2)}{\psi_1^{\theta_B}(\xi_0, 3\Sigma_{s0}R/2)}, \quad (14)$$

where (13) and (14) are identical when $\xi_0 = 0$. For consistency with Becker & Coppens (1974), $\Sigma_{s0}R$ is used as a variable for the reduced radius in Y_ν and Y_μ.

(*b*) A better approximation is to consider the sphere as a stack of cylindrical platelets with equal thickness dz and different radius ρ, parallel to the plane of diffraction defined by the incident and diffraction vectors (see Fig. 5). Then the multiple IRPR of each cylindrical platelet

can be approximated as the diffraction from a plane platelet and a mean path length of $16\rho/3\pi$ with an incident beam of area $2\rho\,dz$, which gives a contribution of $2R_H^{\theta}[\xi_0, 16\Sigma_{s0}(R^2 - z^2)^{1/2}/3\pi](R^2 - z^2)^{1/2}\,dz$.

The corresponding IRPRs for single reflection by non-absorbing and absorbing spherical crystals are, respectively,

$$(Q/\eta)\int_0^R (16\rho/3\pi)4\rho\,dz = (64Q/3\pi\eta)\int_0^R (R^2 - z^2)\,dz = 128 \times 2^{1/2}\Sigma_{s0}R^3/9\pi^{1/2} \tag{15}$$

and

$$\psi_2^0(\xi_0, \Sigma_{s0}R) = 4\int_0^R (QA_c^0/\eta)[\xi_0, 16\Sigma_{s0}(R^2 - z^2)^{1/2}/3\pi] \times (R^2 - z^2)^{1/2}\,dz \tag{16}$$

$$\psi_2^{\pi/2}(\xi_0, \Sigma_{s0}R) = 4\int_0^R (QA_c^{\pi/2}/\eta)[\xi_0, 16\Sigma_{s0}(R^2 - z^2)^{1/2}/3\pi] \times (R^2 - z^2)^{1/2}dz. \tag{17}$$

The IRPRs for multiple reflection are

$$\phi_2^0(\xi_0, \Sigma_{s0}R) = 4\int_0^R (R_H^{\theta, 0}/\eta)[\xi_0, 16\Sigma_{s0}(R^2 - z^2)^{1/2}/3\pi] \times (R^2 - z^2)^{1/2}\,dz \tag{18}$$

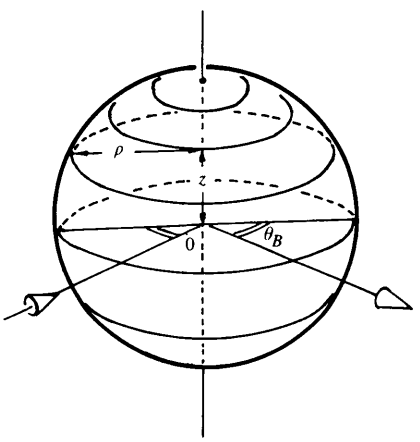

Fig. 5. The cylindrical coordinate system (z, ρ). z and ρ are related by $\rho^2 + z^2 = R^2$.

$$\phi_2^{\pi/2}(\xi_0, \Sigma_{s0}R) = 4\int_0^R (R_H^{\theta, \pi/2}/\eta)[\xi_0, 16\Sigma_{s0}(R^2 - z^2)^{1/2}/3\pi] \times (R^2 - z^2)^{1/2}\,dz. \tag{19}$$

Then, $\phi_2^{\theta_B}$ and $\psi_2^{\theta_B}$ can be approximated as in the right sides of (9) and (10), respectively.

Thus, we obtain the expressions

$$Y_\nu(\xi_0, \Sigma_{s0}R, \theta_B) = \frac{9\pi^{1/2}\phi_2^{\theta_B}(\xi_0, \Sigma_{s0}R)}{128 \times 2^{1/2}\Sigma_{s0}R^3} \tag{20}$$

$$Y_\mu(\xi_0, \Sigma_{s0}R, \theta_B) = \frac{\phi_2^{\theta_B}(\xi_0, \Sigma_{s0}R)}{\psi_2^{\theta_B}(\xi_0, \Sigma_{s0}R)}. \tag{21}$$

(*c*) The third method is to consider the sphere just as a sphere. The corresponding IRPRs for single reflection by a real absorbing spherical crystal can be expressed by ψ_3:*

$$\psi_3 = (QA/\eta)V, \tag{22}$$

where V is the volume of the sphere and A is the transmission coefficient. From *ITXCr* (1972), the exact expressions of A for $\theta_B = 0$ and $\theta_B = \pi/2$ are

$$A^0 = [3/2(\mu R)^3]\{\tfrac{1}{2} - \exp(-2\mu R) \times [\tfrac{1}{2} + \mu R + (\mu R)^2]\} \tag{23}$$

$$A^{\pi/2} = (3/4\mu R)\{\tfrac{1}{2} - [1/16(\mu R)^2][1 - (1 + 4\mu R) \times \exp(-4\mu R)]\}. \tag{24}$$

Hence,

$$\psi_3^0(\xi_0, \Sigma_{s0}R) = [(8\pi^3)^{1/2}/\Sigma_{s0}^2\xi_0^3]\{\tfrac{1}{2} - \exp(-2\xi_0\Sigma_{s0}R) \times [\tfrac{1}{2} + \xi_0\Sigma_{s0}R + (\xi_0\Sigma_{s0}R)^2]\} \tag{25}$$

$$\psi_3^{\pi/2}(\xi_0, \Sigma_{s0}R) = [(2\pi^3)^{1/2}(\Sigma_{s0}R)^2/\Sigma_{s0}^2\xi_0] \times \{\tfrac{1}{2} - [1/16(\xi_0\Sigma_{s0}R)^2] \times [1 - (1 + 4\xi_0\Sigma_{s0}R) \times \exp(-4\xi_0\Sigma_{s0}R)]\}. \tag{26}$$

* The following formulae should be used instead of (22) and (25) when $\xi_0\Sigma_{s0}R < 0.02$:

(i) the IRPR for single reflection by an absorbing cylindrical platelet:

$$2\rho(QA_c^0/\eta)\,dz = 4(2\pi)^{1/2}\Sigma_{s0}\rho^2\int_0^{\pi/2} \exp(-2\xi_0\Sigma_{s0}\rho\cos\phi) \times \cos^2\phi\,d\phi\,dz;$$

(ii) the corresponding IRPR for single reflection by an absorbing spherical crystal:

$$\psi_3^0(\xi_0, \Sigma_{s0}R) = 4\int_0^R (QA_c^0/\eta)[\xi_0, \Sigma_{s0}(R^2 - z^2)^{1/2}](R^2 - z^2)^{1/2}\,dz.$$

For calculating the IRPR for multiple reflection, the sphere is again considered as a stack of cylindrical platelets. Following Hamiliton (1957), the diffraction by a cylindrical platelet can be considered as being composed of an infinite number of pencil beams with different path length in a platelet. Here the exact values of IRPR for multiple reflection of each platelet at $\theta_B = 0$ and $\pi/2$ can be calculated for both absorbing and non-absorbing cases; thus, the exact value of R_H^θ for a spherical crystal for $\theta_B = 0$ and $\pi/2$ can also be evaluated.

The corresponding IRPR for multiple reflection by a cylindrical platelet is

$$2\rho(R_H^\theta/\eta)(\xi_0, \Sigma_{s0}\rho)\,\mathrm{d}z = 2\rho \int_0^{\pi/2} \int_{-\infty}^{\infty} (P_H/P_0)(\xi, 2\Sigma_s\rho\cos\varphi) \times \cos\varphi\,(\mathrm{d}\Delta\theta/\eta)\,\mathrm{d}\varphi\,\mathrm{d}z. \quad (27)$$

The IRPR for a cylindrical platelet under $\theta_B = \pi/2$ and 0 when $\xi_0 \neq 0$ can be calculated by substituting (6) to (8) into (27), respectively. And, when $\xi_0 = 0$, they can be calculated by substituting (7) and (8) into (27), respectively. By transforming the variable from ρ into z, the IRPR for multiple reflection by a spherical crystal is

$$\phi_3^0(\xi_0, \Sigma_{s0}R) = 4\int_0^R (R_H^{\theta,0}/\eta)[\xi_0, \Sigma_{s0}(R^2 - z^2)^{1/2}] \times (R^2 - z^2)^{1/2}\,\mathrm{d}z \quad (28)$$

$$\phi_3^{\pi/2}(\xi_0, \Sigma_{s0}R) = 4\int_0^R (R_H^{\theta,\pi/2}/\eta)[\xi_0, \Sigma_{s0}(R^2 - z^2)^{1/2}] \times (R^2 - z^2)^{1/2}\,\mathrm{d}z. \quad (29)$$

Then, $\phi_3^{\theta_B}$ and $\psi_3^{\theta_B}$ can be approximated as in the right sides of (9) and (10). Thus, we obtain the expressions

$$Y_\nu(\xi_0, \Sigma_{s0}R, \theta_B) = \frac{3\phi_3^{\theta_B}(\xi_0, \Sigma_{s0}R)}{4(2\pi^3)^{1/2}\Sigma_{s0}R^3} \quad (30)$$

$$Y_\mu(\xi_0, \Sigma_{s0}R, \theta_B) = \frac{\phi_3^{\theta_B}(\xi_0, \Sigma_{s0}R)}{\psi_3^{\theta_B}(\xi_0, \Sigma_{s0}R)}. \quad (31)$$

From (25)–(29), we note that both ψ_3 and ϕ_3 are proportional to $1/\Sigma_{s0}^2$. Thus, the ratio between them, Y_μ, is only a function of ξ_0 and $\Sigma_{s0}R$.

In the supplementary data,* tables list the values of ϕ_3^0 and $\phi_3^{\pi/2}$ for different ξ_0 and $\Sigma_{s0}R$. These tables were calculated based on an arbitrarily chosen $\Sigma_{s0} = 40.0\,\mathrm{cm}^{-1}$. Thus, for calculating Y_ν or Y_μ, the same value of Σ_{s0} should be used for the denominator of (30) and (31).

The IRPR and hence the Y_ν, Y_μ derived from the three different methods may deviate from each other quite appreciably in some cases. We take the extreme case $\theta_B = 0$ as an important example.

For $\theta_B = 0$ and when absorption is very low, *i.e.* $\xi_0 \simeq 0$, the values of IRPR for multiple reflection as well as Y_μ derived from the three methods are similar. However, for the case of $\xi_0 > 0.5$ and $\xi_0\Sigma_{s0}R > 1.5$ (*i.e.* $R > 1.5/\mu$), the situation changes drastically. Physically, the increase of ξ_0 or $\Sigma_{s0}R$ means the increase of the opacity at the center region of the sphere and the slow movement of the main part of the exit diffracted beam toward the periphery of the sphere. For the single-plate approximation (*a*), this effect is completely overlooked. For method (*b*), only the exit diffracted beam close to the polar region of the sphere along the z direction is considered, while the penetration of the diffracted beam around the periphery other than the polar region is still overlooked. Only method (*c*), the exact approach, considers all these effects. Thus, for example, the IRPR calculated from method (*b*) for $\xi_0 = 1$, $\Sigma_{s0}R = 6$ and $\theta_B = 0$ is 16.8 times larger than that from (*a*), while method (*c*) gives an IRPR value 4.3 times larger than that from (*b*). Fig. 6 depicts the dependence of Y_μ on $\Sigma_{s0}R$ at $\theta_B = 0$ from the three different methods. Method (*a*) gives a curve similar to the curve for a plane crystal for the symmetric Laue case (see Fig. 2), with $A_{k0} = 3\Sigma_{s0}R/2$, but both methods (*b*) and (*c*) give higher values of Y_μ for the same $\Sigma_{s0}R$. This is because, for a defined $\Sigma_{s0}R$, the equivalent mean path length of the cylinder plate for method (*b*) contributing to the main part of the diffracted beam of the sphere will decrease with increasing ξ_0, and this in turn will lead to the increase of Y_μ. The Y_μ from method (*c*) is larger since in this method more periphery effect has been considered. Y_ν is nearly the same from the three different methods, the Y_ν *versus* $\Sigma_{s0}R$ curve is similar to that of a plane crystal under symmetric Laue geometry (see Fig. 1) if $3\Sigma_{s0}R/2$ is used instead of A_k as the abscissa. These curves decrease very quickly at large ξ_0. This diffraction behavior is similar to that under small θ_B.

Y_ν or Y_μ is nearly the same from the three methods for $\theta_B = \pi/2$. Fig. 7 depicts the dependence of $\Sigma_{s0}R$ on the exact values of Y_μ for $\theta_B = 0$ and $\theta_B = \pi/2$.

For a non-absorbing crystal, when $\sin\theta_B = 0.05$, the Y_ν (or Y_μ) are 0.1445, 0.0808 and 0.0308 for $\Sigma_{s0}R = 5$, 10 and 30, respectively; while the corresponding values given by Becker & Coppens (1974) (BC) are 0.1476, 0.0802 and 0.0256. The difference between the results from this work and those from BC is 18% for $\Sigma_{s0}R = 30$. One can see from Fig. 8(*a*) that our secondary-extinction factor Y_ν for $\theta_B = \pi/6$, $\mu = 0$ calculated by method (*c*) is in good agreement with those of BC. The Y_ν are 7.9 and 5.9% smaller than BC at $\Sigma_{s0}R = 5$ and

* Tables of ϕ_3^0 and $\phi_3^{\pi/2}$ have been deposited with the IUCr (Reference: CR0503). Copies may be obtained through The Managing Editor, International Union of Crystallography, 5 Abbey Square, Chester CH1 2HU, England.

30, respectively. For $\xi_0 = 1$, $\Sigma_{s0}R < 3$, the maximum difference of Y_μ between our result and that of BC is 5.3%, while the value given by Zachariasen (1967) is 11.6% larger than ours.

We note that a dip always appears in the Y_μ *versus* Σ_{s0} curves when $\xi_0 > 0.1$, as shown in Fig. 8(*c*). This seems reasonable when the Y_μ *versus* A_{k0} curves for a crystal plate under symmetric Bragg and Laue cases, as shown in Fig. 2, are examined, since the diffraction geometry for a spherical crystal is assumed to be a combination of the two cases. However, in BC and Zachariasen's curves almost no dip appears. We also note that the Y_μ for a spherical crystal approaches the corresponding saturated value for a plane crystal under Bragg geometry for $\theta_B = \pi/6$, $\xi_0\Sigma_{s0}R > 10$, *i.e.* when $R > 10/\mu$. This also seems reasonable.

In comparing the observed extinction factor with the calculated secondary-extinction factor Y_μ, one should note that the observed integrated reflecting power ρ_i is

$$\rho_i = F_o^2 \, \mathrm{Lp} \, A, \tag{32}$$

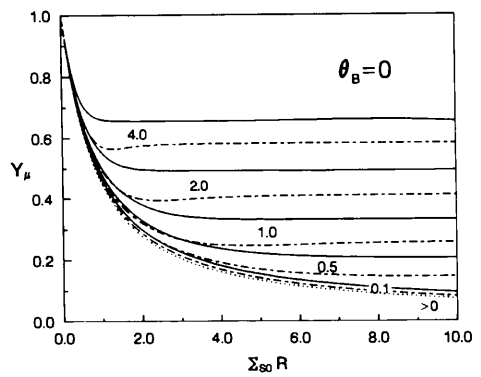

Fig. 6. The secondary-extinction factor Y_μ for a spherical mosaic crystal under $\theta_B = 0$ as a function of $\Sigma_{s0}R$ for different values of ξ_0. Method (*a*) dotted curve; method (*b*) dash-dotted curve; method (*c*) continuous curve.

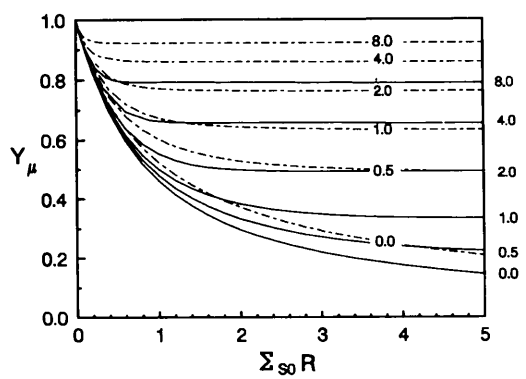

Fig. 7. The secondary-extinction factor Y_μ for a spherical mosaic crystal calculated by method (*c*) as a function of $\Sigma_{s0}R$. $\theta_B = 0$ continuous curve; $\theta_B = \pi/2$ dash-dotted curve. The parameters given on the curves are for ξ_0.

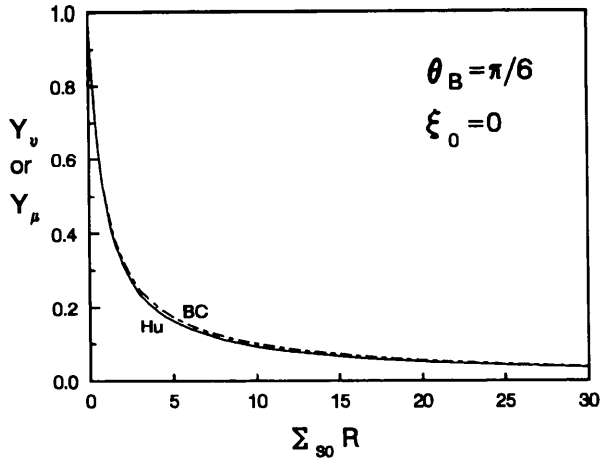

(*a*)

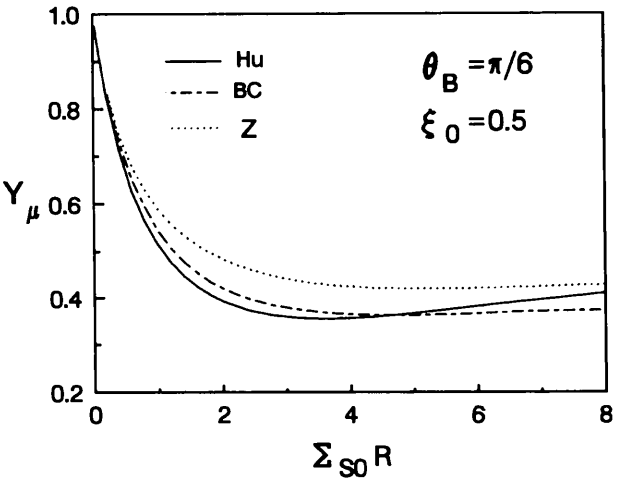

(*b*)

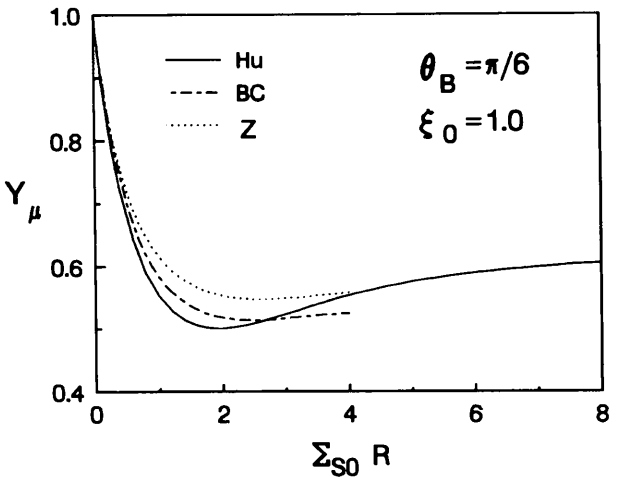

(*c*)

Fig. 8. Comparison of Y_μ calculated by method (*c*) at $\theta_B = \pi/6$ with the results given by Becker & Coppens (1974) and Zachariasen (1967) stopping at $\xi_0\Sigma_{s0}R = 4$, beyond which no $\bar{T}\mu$ value (Rigoult & Guidi-Morosini, 1980) is available for calculation.

where Lp is the Lorentz–polarization factor and A is the transmission coefficient for a spherical crystal, which is a function of θ_B and μR (*International Tables for Crystallography*, 1995) (*ITCr*). The observed extinction factor Y_o can be evaluated through $Y_o = F_o^2/F_c^2$, where F_o is the observed structure amplitude.

3. Application of the theory of extinction to a real plane crystal

In most of the real single-crystal cases, even the nature of the extinction, *i.e.* primary or secondary type, has remained confused until now. To demonstrate the applicability of our extinction theory to a crystal plate, we take two examples. For LiF single crystals, extinction is a problem that has been debated for more than 20 years (Zachariasen, 1968; *L*1972; Killean, Lawrence & Sharma, 1972; Becker & Coppens, 1974). The other example is MgO, which exhibits very strong extinction. The extinction factor for some of its reflections can be as low as ~ 0.05 (*L*1973*b*) and so its treatment becomes very difficult.

3.1. *LiF single crystal*

All the original experimental data of LiF are taken directly from the original publications (*L*1972; *L*1973*a*,*b*). The atomic scattering factors are from *ITXCr* (1974). The very small anomalous-dispersion correction is neglected. Lawrence measured the IRPR of 46 sets of symmetry-equivalent reflections, corresponding to about 100 b values, for a large plane LiF single crystal (NaCl structure, $a = 4.0262$ Å, $t_o = 0.139$ cm, with Mo $K\alpha$ X-radiation, $\lambda = 0.7107$ Å, $\mu = 3.4\ \text{cm}^{-1}$). The results are listed in Table 1 in which:

(i) The calculated $\bar{Y}_c$ is the mean value of Y_μ for all the equivalent reflections for different Bragg and Laue cases. For example, the reflection 331 includes four Laue cases with $b = 2.307$, 0.4333, 1.218 and 0.8210, giving $A_c = 0.0656$, 0.1514, 0.0828, 0.1009; the value of Y_c for the first two reflections is 0.914 and for the latter two is 0.942, and thus $\bar{Y}_c = 0.928$ is the overall mean value.

(ii) All the reflections were simultaneously included in the fitting process. A revised scale factor of 1.1 and three fitting parameters, $\eta = 0.58'$, $B_{\text{Li}} = 1.02$ and $B_F = 0.655$ Å^2 were used throughout the analysis. The R factor

$$R = \sum ||F_o| - |F_c|| \Big/ \sum |F_o|$$

and $\sum |\Delta Y|/N$, where N is the number of sets of symmetry-equivalent reflections evaluated here, have the values $R = 0.0137$ and $\sum |\Delta Y|/N = 0.0158$. This shows that the agreement is very satisfactory, particularly when one considers that all the reflections are included. We also note that (i) the fitting parameter $\eta = 0.58'$ corresponding to a FWHM of $82''$ is much larger than the $2.3''$ Darwin width for the 200 reflection and (ii) the radius of the mosaic block $r \simeq 2 \times 10^{-6}$ m measured by Killean *et al.* (1972) through the dislocation density is much less than the extinction distance $\Lambda = 1.2 \times 10^{-5}$ m for the 200 reflection with $\lambda = 0.7107$ Å. All these suggest that extinction of LiF is of the secondary type, in agreement with Killean, Lawrence & Sharma (1972) who used the same batch of LiF crystals as Lawrence, and not the primary type as Lawrence (1972) and Becker & Coppens (1974) claimed.

Table 1. *The structure factor observed, F_o, corrected, $F_o^l = F_o/\bar{Y}_c^{1/2}$, and calculated, F_c; and the extinction factor observed, Y_o, and calculated, $\bar{Y}_c$, for each reflection of LiF*

h	k	l	F_o	F_o^l	F_c	Y_o	$\bar{Y}_c$
1	1	1	9.88	19.07	19.07	0.268	0.268
2	0	0	13.09	30.18	29.13	0.202	0.188
2	2	0	12.21	20.57	20.82	0.344	0.352
3	1	1	7.55	8.84	8.71	0.752	0.729
2	2	2	11.17	15.25	16.03	0.485	0.536
4	0	0	10.63	12.62	12.95	0.674	0.710
3	3	1	5.55	5.76	5.75	0.930	0.928
4	2	0	9.47	10.95	10.82	0.766	0.749
4	2	2	8.35	9.29	9.26	0.812	0.808
5	1	1	4.51	4.60	4.52	0.996	0.963
4	4	0	6.79	7.10	7.16	0.899	0.912
5	3	1	3.80	3.85	3.85	0.971	0.970
6	0	0	6.14	6.30	6.41	0.916	0.949
4	4	2	6.13	6.34	6.41	0.912	0.933
6	2	0	5.55	5.67	5.80	0.915	0.957
5	3	3	3.36	3.40	3.42	0.964	0.976
6	2	2	5.09	5.19	5.29	0.925	0.962
4	4	4	4.69	4.78	4.85	0.933	0.961
5	5	1	3.04	3.07	3.09	0.971	0.984
7	1	1	3.05	3.07	3.09	0.978	0.990
6	4	0	4.36	4.43	4.48	0.951	0.972
6	4	2	4.08	4.13	4.14	0.969	0.975
8	0	0	3.54	3.57	3.59	0.976	0.988
7	3	3	2.53	2.54	2.56	0.977	0.992
8	2	0	3.32	3.35	3.35	0.985	0.988
6	6	0	3.13	3.15	3.13	0.994	0.986
8	2	2	3.14	3.15	3.13	1.001	0.989
7	5	1	2.31	2.32	2.33	0.981	0.991
6	6	2	2.94	2.96	2.94	0.999	0.987
8	4	0	2.78	2.80	2.76	1.017	0.989
7	5	3	2.12	2.13	2.12	0.998	0.991
9	1	1	2.11	2.11	2.12	0.989	0.995
8	4	2	2.59	2.61	2.59	1.001	0.989
6	6	4	2.43	2.45	2.44	0.998	0.986
9	3	1	1.91	1.92	1.93	0.981	0.993
8	4	4	2.16	2.17	2.16	1.001	0.989
7	5	5	1.74	1.75	1.75	0.990	0.993
7	7	1	1.74	1.75	1.75	0.990	0.993
10	0	0	2.03	2.04	2.04	1.000	0.992
8	6	0	2.03	2.04	2.04	1.000	0.991
10	2	0	1.89	1.90	1.92	0.967	0.990
8	6	2	1.91	1.92	1.92	0.989	0.991
9	5	1	1.54	1.55	1.59	0.944	0.993
7	7	3	1.55	1.56	1.59	0.957	0.991
10	2	2	1.78	1.79	1.81	0.969	0.990
6	6	6	1.79	1.80	1.81	0.980	0.991

3.2. *MgO single crystal*

For a detailed analysis of the very strong extinction in X-ray diffraction by an MgO single-crystal plate, the original experimental data of Lawrence (1973*b*)

are used. MgO has the NaCl structure ($a = 4.213$ Å, $t_0 = 0.151$ cm) with Mo $K\alpha$ X-radiation ($\lambda = 0.7107$Å), $\mu = 10.2\,\text{cm}^{-1}$. All the $N'(N' = 77)$ sets of Laue and Bragg cases for symmetry-equivalent reflections were listed and reanalyzed separately. During the analysis we found:

(i) When secondary extinction is considered alone, the best fit ($\eta = 0.052'$, $B_{\text{Mg}} = 0.30$, $B_{\text{O}} = 0.345$ Å^2) gives rather large values, $R = 0.103$, $\sum|\Delta Y|/N' = 0.0592$. There is a systematic deviation between the calculated values for the Bragg and Laue cases and the corresponding data cannot be matched by adjusting the parameters. These results indicate the existence of primary extinction that should be calculated together with secondary extinction.

(ii) For this purpose, $\Sigma_{s0}Y_p$ is inserted into (2) instead of Σ_{s0} (Werner, 1974). The primary-extinction factor Y_p is calculated by the method of Becker & Coppens (1974), and the readjusted parameters after the introduction of both primary and secondary extinction are $\eta = 0.20'$, $r = 38\,\mu$m. The Debye–Waller factors $B_{\text{Mg}} = 0.30$, $B_{\text{O}} = 0.34$ Å^2 are identical with Lawrence's (1973*a*) fit for his small MgO spherical-crystal case. The results for the extinction factor and some related parameters for both the Laue case and the Bragg case are listed in Tables 2 and 3, respectively. Just as in the LiF case, the minimum value of the R factor and of $\sum|\Delta Y|/N'$ is obtained by manual adjustment without the use of a least-squares program. The final results, $R = 0.0533$, $\sum|\Delta Y|/N' = 0.0376$, show a noticeable improvement compared to results for secondary-extinction correction alone.

Note that several columns of the parameters after Y_p in Table 2 and Table 3 where primary extinction is involved are obtained by putting $Y_p\Sigma_{s0}$ instead of Σ_{s0} in the numerator. Also, Y_{sc} (corrected only for secondary extinction) for different b are listed separately, while for b and $1/b$ there is only one value presented since the Y_{sc} are the same. $\bar{Y}_{sc}$ is the mean value of Y_{sc} for different b. Values of Y_c, $\bar{Y}_c$ are extinction factors with both primary and secondary extinction considered.

The value $Y = Y_pY_s$ has been used occasionally when both primary and secondary extinction exists. However, such an approximation agrees with our result only for $Y_p > 0.8$ (see Tables 2, 3). For $Y_p < 0.8$, our treatment gives a Y_c value larger than Y_pY_s and the deviation increases further for small Y_p. This is why we use Werner's treatment instead of using the value Y_pY_s. The value $r = 38\,\mu$m may be slightly too large in comparison with the result of $L(1973b)$ for MgO but our purpose here is not to determine the value of r but to explain why a small primary-extinction factor at low-angle reflection is required for a good fit. The ultimate test of the validity of this method will require experiment with different values of λ.

The values of Y_ν for the MgO 200 reflection evaluated with the same R_H^θ, A_{k0} and η value listed in Tables 2 and 3 for the Laue and Bragg cases are 0.0042 and 0.0019, respectively. The values of Y_ν for the 933 reflection are 0.034 and 0.22 for the Laue and Bragg cases, respectively. One can see that in an absorbing crystal the values of Y_ν for Bragg geometry remain small even for a very large reflection angle such as $\sin\theta_B/\lambda = 1.18$ Å^{-1}. This means that the scaling factor would be inaccurate if Y_ν were used for data reduction in such a case.

There are several factors that make the R value for MgO larger than for LiF. The first is the very strong extinction in MgO, in which most of the observed extinction factors for the Bragg case are larger than for the corresponding Laue case. Thus, $L(1973b)$ listed them separately but in LiF the listed values are the mean for the two cases, which is easier to fit than if they are treated separately. $L(1973b)$ remarked in his MgO work: 'The observed structure factors for a set of symmetry-equivalent reflections whose planes diffracted with Laue-type geometry were the same, as were those with Bragg type'. However, from Tables 2 and 3, one can see that for a set of symmetry-equivalent reflections the calculated structure factor usually will be different for different b. The difference in some cases may be as large as 20%. The co-existence of primary and secondary extinction in MgO also makes the fit more difficult.

From the above analysis, one can see that it is necessary, for an accurate determination of the structure factor from a single-crystal sample, to ensure that:

(*a*) The sample is of good quality with homogeneous mosaic spread throughout and free from any deformation. Its surface should be properly treated by mild etching and the size of the plane crystal should be large enough to cover all the reflected beam with the reception width of the detector sufficiently wide. It is also desirable to make a preliminary test run to estimate the mosaic spread of the sample to see if the thickness of the sample is reasonable.

(*b*) When a set of symmetry-equivalent reflections for a plane crystal is measured, it is desirable to treat the Bragg and Laue cases for different b values separately. For an absorbing plane crystal, it is better to analyze the same set of data with both Y_ν and Y_μ, considering that Y_ν decreases with increasing ξ_0 and Y_μ increases with increasing ξ_0 (see Figs. 1 and 2). The agreement between the values of F_{cor} obtained from the two Y_s's can be used as a criterion for the correctness of the chosen scaling factor, η, and the Debye–Waller factors.

4. Conclusions and discussion

The re-analysis of the experiments LiF and MgO yield very good fits, showing that simple, exact and universal expressions for the secondary extinction for a crystal plate can be obtained and can be extended to the spherical crystal with satisfactory results. Hereafter, all seriously extinguished reflections in single-crystal diffractometry may be accessible for data analysis in

Table 2. *The observed and calculated structure factors and the observed and calculated extinction factor for each Laue reflection of MgO*

The values of Q (rad cm^{-1}) and R_H^θ are multiplied by 10^4.

h	k	l	θ_B	F_o	F_c	Q	b	A_c	Y_o	Y_{sc}	$\bar{Y}_{sc}$	Y_p	ξ_0	A_{k0}	R_H^θ	Y_c	$\bar{Y}_c$
2	0	0	9.71	8.40	52.52	399.5	1.00	0.032	0.026	0.030	0.030	0.071	0.522	2.99	0.2555	0.020	0.020
2	2	0	13.80	8.45	41.17	166.5	0.61	0.028	0.042	0.048	0.056	0.097	0.918	3.24	0.1494	0.032	0.036
							1.00	0.032		0.064				1.73	0.2114	0.040	
2	2	2	16.99	8.44	33.93	88.62	0.64	0.032	0.062	0.092	0.092	0.126	1.331	1.89	0.1615	0.057	0.057
4	0	0	19.72	8.42	28.89	53.46	1.00	0.031	0.085	0.164	0.164	0.158	1.762	0.93	0.1519	0.091	0.091
4	2	0	22.16	8.48	25.17	34.95	0.66	0.034	0.114	0.209	0.196	0.192	2.213	1.06	0.1361	0.115	0.110
							0.10	0.014		0.151				9.06	0.0464	0.094	
							1.00	0.031		0.228				0.75	0.1310	0.121	
4	2	2	24.41	8.32	22.32	24.20	0.66	0.034	0.139	0.277	0.252	0.229	2.682	0.87	0.1218	0.149	0.139
							0.22	0.021		0.226				3.05	0.0659	0.129	
4	4	0	28.50	8.36	18.24	13.11	0.30	0.027	0.210	0.369	0.404	0.307	3.691	1.47	0.0730	0.204	0.215
							1.00	0.030		0.439				0.47	0.0883	0.226	
6	0	0	30.40	7.81	16.73	10.11	1.00	0.029	0.218	0.504	0.504	0.347	4.235	0.42	0.0783	0.264	0.264
4	4	2	30.40	8.17	16.73	10.11	0.31	0.029	0.239	0.437	0.437	0.347	4.235	1.19	0.0704	0.243	0.251
							0.66	0.033		0.486				0.56	0.0872	0.259	
6	2	0	32.24	7.73	15.46	8.00	0.65	0.033	0.250	0.545	0.554	0.387	4.808	0.51	0.0782	0.297	0.299
							1.00	0.029		0.562				0.38	0.0697	0.301	
6	2	2	34.02	7.51	14.38	6.48	0.65	0.033	0.273	0.597	0.597	0.425	5.408	0.46	0.0703	0.334	0.334
4	4	4	35.76	7.66	13.45	5.35	0.33	0.030	0.324	0.605	0.605	0.461	6.032	0.79	0.0570	0.357	0.357
6	4	0	37.46	7.47	12.64	4.51	0.32	0.030	0.349	0.646	0.668	0.495	6.674	0.71	0.0524	0.391	0.399
							1.00	0.027		0.690				0.29	0.0501	0.407	
6	4	2	39.14	7.10	11.94	3.86	0.32	0.029	0.354	0.681	0.694	0.526	7.326	0.66	0.0482	0.424	0.429
							0.63	0.031		0.708				0.36	0.0519	0.434	
8	0	0	42.44	6.51	10.75	2.98	1.00	0.025	0.367	0.761	0.761	0.580	8.609	0.24	0.0372	0.492	0.492
8	2	0	44.07	6.43	10.25	2.68	0.61	0.029	0.394	0.768	0.772	0.602	9.213	0.32	0.0395	0.511	0.513
							1.00	0.025		0.776				0.23	0.0340	0.515	
6	4	4	44.07	6.42	10.25	2.68	0.30	0.028	0.393	0.751	0.751	0.602	9.213	0.57	0.0375	0.503	0.503
6	6	0	45.70	6.61	9.79	2.45	1.00	0.024	0.455	0.787	0.787	0.622	9.774	0.23	0.0311	0.534	0.534
8	2	2	45.70	6.71	9.79	2.45	0.60	0.028	0.469	0.780	0.780	0.622	9.774	0.31	0.0363	0.531	0.531
6	6	2	47.33	6.39	9.38	2.26	0.59	0.027	0.465	0.789	0.789	0.640	10.27	0.31	0.0335	0.548	0.548
8	4	0	48.97	6.23	8.99	2.12	0.27	0.025	0.480	0.786	0.794	0.655	10.71	0.58	0.0297	0.557	0.561
							1.00	0.023		0.801				0.22	0.0264	0.564	
8	4	2	50.63	6.24	8.64	2.02	0.26	0.024	0.522	0.793	0.796	0.668	11.05	0.60	0.0275	0.569	0.571
							0.57	0.025		0.799				0.31	0.0288	0.573	
6	6	4	52.30	6.06	8.32	1.94	0.24	0.023	0.531	0.796	0.796	0.679	11.31	0.63	0.0256	0.579	0.579
8	4	4	55.73	6.10	7.73	1.85	0.21	0.020	0.624	0.798	0.798	0.697	11.52	0.76	0.0222	0.593	0.593
10	0	0	57.51	5.73	7.46	1.84	1.00	0.016	0.590	0.791	0.791	0.703	11.47	0.25	0.0175	0.594	0.594
8	6	0	57.51	5.95	7.46	1.84	1.00	0.016	0.636	0.791	0.791	0.703	11.47	0.25	0.0175	0.594	0.594
10	2	0	59.34	5.75	7.20	1.85	0.50	0.018	0.636	0.780	0.780	0.709	11.31	0.41	0.0193	0.592	0.592
							1.00	0.014		0.781				0.27	0.0159	0.593	
8	6	2	59.34	5.83	7.20	1.85	0.50	0.018	0.654	0.780	0.780	0.709	11.31	0.41	0.0193	0.592	0.592
10	2	2	61.23	5.71	6.96	1.89	0.47	0.016	0.671	0.768	0.768	0.714	11.04	0.46	0.0174	0.589	0.589
10	4	0	65.29	5.34	6.52	2.03	0.07	0.013	0.671	0.763	0.743	0.722	10.15	2.99	0.0151	0.590	0.579
							1.00	0.010		0.724				0.36	0.0105	0.568	
10	4	2	67.51	5.08	6.31	2.16	0.03	0.011	0.647	0.745	0.727	0.725	9.516	8.66	0.0137	0.582	0.571
							0.38	0.010		0.709				0.78	0.0112	0.560	
3	3	1	21.57	6.03	9.73	5.40	0.45	0.030	0.384	0.604	0.641	0.513	5.361	0.68	0.0618	0.387	0.401
							0.83	0.033		0.677				0.35	0.0745	0.415	
5	1	1	25.99	5.43	7.28	2.37	0.83	0.033	0.556	0.829	0.829	0.663	9.475	0.20	0.0452	0.584	0.584
5	3	1	29.93	4.74	5.51	1.12	0.49	0.033	0.739	0.896	0.893	0.784	16.93	0.18	0.0265	0.719	0.717
							0.82	0.032		0.910				0.12	0.0260	0.728	
							0.05	0.018		0.871				2.19	0.0142	0.703	
5	3	3	33.58	3.85	4.26	0.58	0.49	0.033	0.817	0.944	0.938	0.866	29.78	0.11	0.0155	0.824	0.819
							0.12	0.022		0.933				0.44	0.0106	0.815	
7	1	1	37.04	3.17	3.37	0.32	0.81	0.030	0.886	0.971	0.971	0.916	50.22	0.04	0.0086	0.891	0.891
5	5	1	37.04	3.19	3.37	0.32	0.15	0.024	0.898	0.962	0.966	0.916	50.22	0.21	0.0070	0.884	0.887
							0.81	0.030		0.971				0.04	0.0086	0.891	
7	3	1	40.38	2.61	2.73	0.20	0.47	0.031	0.910	0.979	0.980	0.945	79.65	0.04	0.0056	0.926	0.927
							0.80	0.029		0.981				0.03	0.0053	0.928	
5	5	3	40.38	2.60	2.73	0.20	0.16	0.025	0.903	0.977	0.978	0.945	79.65	0.12	0.0045	0.924	0.925
							0.47	0.031		0.979				0.04	0.0056	0.926	
7	3	3	43.66	2.19	2.27	0.13	0.45	0.029	0.933	0.985	0.985	0.962	117.4	0.03	0.0037	0.949	0.949

Table 2 *(cont.)*

h	k	l	θ_B	F_o	F_c	Q	b	A_c	Y_o	Y_{sc}	$\bar{Y}_{sc}$	Y_p	ξ_0	A_{k0}	R_H^θ	Y_c	$\bar{Y}_c$
7	5	1	46.92	1.86	1.93	0.10	0.14	0.024	0.926	0.988	0.989	0.972	159.9	0.07	0.0022	0.961	0.962
							0.78	0.026		0.990				0.02	0.0024	0.962	
9	1	1	50.21	1.68	1.68	0.08	0.77	0.024	0.994	0.991	0.991	0.978	200.9	0.01	0.0017	0.970	0.970
7	5	3	50.21	1.72	1.68	0.08	0.12	0.022	1.043	0.991	0.991	0.978	200.9	0.07	0.0016	0.969	0.969
							0.41	0.025		0.991				0.02	0.0019	0.969	
9	3	1	53.57	1.46	1.50	0.06	0.38	0.023	0.957	0.992	0.992	0.982	233.2	0.02	0.0014	0.974	0.974
							0.75	0.021		0.992				0.01	0.0013	0.974	
7	7	1	57.06	1.31	1.36	0.06	0.73	0.018	0.932	0.992	0.992	0.984	250.9	0.01	0.0010	0.976	0.976
9	3	3	57.06	1.35	1.36	0.06	0.34	0.020	0.990	0.992	0.992	0.984	250.9	0.02	0.0012	0.976	0.976

Table 3. *The observed and calculated structure factors and the observed and calculated extinction factors for each Bragg reflection of MgO*

The values of Q (rad cm^{-1}) and R_H^θ are multiplied by 10^4.

h	k	l	θ_B	F_o	F_c	Q	b	A_c	Y_o	Y_{sc}	$\bar{Y}_{sc}$	Y_p	ξ_0	A_{k0}	R_H^θ	Y_c	$\bar{Y}_c$
2	0	0	9.71	12.24	52.52	399.5	−1.00	0.049	0.054	0.101	0.101	0.071	0.522	17.50	0.6910	0.035	0.035
4	0	0	19.72	11.19	28.89	53.46	−1.00	0.049	0.150	0.367	0.367	0.158	1.762	2.59	0.3058	0.117	0.117
6	0	0	30.40	9.73	16.73	10.11	−1.00	0.049	0.338	0.708	0.708	0.347	4.235	0.72	0.1487	0.301	0.301
6	2	0	32.24	9.41	15.46	8.00	−3.24	0.023	0.371	0.744	0.744	0.387	4.808	0.41	0.0627	0.339	0.339
6	2	2	34.02	9.31	14.38	6.48	−5.63	0.015	0.419	0.777	0.777	0.425	5.408	0.33	0.0361	0.377	0.377
6	4	0	37.46	8.59	12.64	4.51	−14.39	0.006	0.462	0.829	0.829	0.495	6.674	0.24	0.0129	0.448	0.448
6	4	2	39.14	8.39	11.94	3.86	−22.79	0.004	0.494	0.849	0.849	0.526	7.326	0.22	0.0076	0.480	0.480
8	0	0	42.44	7.58	10.75	2.98	−1.00	0.049	0.498	0.886	0.886	0.580	8.609	0.27	0.0779	0.539	0.539
8	2	0	44.07	7.51	10.25	2.68	−1.70	0.036	0.538	0.895	0.895	0.602	9.213	0.20	0.0543	0.562	0.562
6	6	0	45.70	7.47	9.79	2.45	−81.78	0.001	0.583	0.898	0.898	0.622	9.774	0.16	0.0017	0.581	0.581
8	2	2	45.70	7.21	9.79	2.45	−2.05	0.032	0.542	0.902	0.902	0.622	9.774	0.17	0.0455	0.582	0.582
8	4	4	55.73	6.47	7.73	1.85	−2.86	0.025	0.702	0.922	0.922	0.697	11.52	0.13	0.0309	0.658	0.658
10	0	0	57.51	6.24	7.46	1.84	−1.00	0.048	0.701	0.928	0.928	0.703	11.47	0.16	0.0587	0.667	0.667
10	2	0	59.34	6.08	7.20	1.85	−1.27	0.042	0.712	0.928	0.928	0.709	11.31	0.14	0.0525	0.672	0.672
8	6	2	59.34	6.12	7.20	1.85	−2.76	0.026	0.722	0.922	0.921	0.709	11.31	0.14	0.0322	0.669	0.668
							−9.81	0.009		0.921				0.15	0.0112	0.668	
10	2	2	61.23	5.94	6.96	1.89	−1.37	0.040	0.727	0.926	0.926	0.714	11.04	0.14	0.0515	0.675	0.675
10	4	0	65.29	5.60	6.52	2.03	−1.45	0.039	0.736	0.921	0.921	0.722	10.15	0.15	0.0539	0.679	0.679
10	4	2	67.51	5.34	6.31	2.16	−1.45	0.039	0.716	0.917	0.917	0.725	9.516	0.16	0.0572	0.680	0.680
5	1	1	25.99	6.06	7.28	2.37	−3.76	0.021	0.692	0.902	0.902	0.663	9.475	0.24	0.0301	0.618	0.618
7	1	1	37.04	3.25	3.37	0.32	−1.73	0.036	0.932	0.985	0.985	0.916	50.22	0.04	0.0104	0.903	0.903
7	3	1	40.38	2.69	2.73	0.20	−3.27	0.023	0.967	0.991	0.991	0.945	79.65	0.02	0.0043	0.937	0.937
7	3	3	43.66	2.24	2.27	0.13	−4.48	0.018	0.976	0.994	0.994	0.962	117.4	0.01	0.0023	0.956	0.956
9	3	1	53.57	1.49	1.50	0.06	−1.70	0.036	0.997	0.997	0.997	0.982	233.2	0.01	0.0023	0.979	0.979
7	7	1	57.06	1.34	1.36	0.06	−4.79	0.017	0.976	0.997	0.997	0.984	250.9	0.01	0.0010	0.981	0.981
9	3	3	57.06	1.35	1.36	0.06	−1.88	0.034	0.990	0.997	0.997	0.984	250.9	0.01	0.0020	0.981	0.981
7	5	5	57.06	1.32	1.36	0.06	−4.79	0.017	0.946	0.997	0.997	0.984	250.9	0.01	0.0010	0.981	0.981
9	5	1	60.75	1.26	1.26	0.06	−1.93	0.033	1.007	0.997	0.997	0.985	250.9	0.01	0.0020	0.982	0.982
7	7	3	60.75	1.23	1.26	0.06	−4.12	0.019	0.959	0.997	0.997	0.985	250.9	0.01	0.0011	0.982	0.982
9	5	3	64.76	1.16	1.18	0.06	−1.88	0.034	0.966	0.997	0.997	0.985	232.9	0.01	0.0021	0.982	0.982
							−17.97	0.005		0.997				0.01	0.0003	0.982	
11	1	1	69.30	1.09	1.12	0.08	−1.10	0.045	0.940	0.997	0.997	0.985	198.1	0.01	0.0034	0.982	0.982
7	7	5	69.30	1.08	1.12	0.08	−2.73	0.026	0.923	0.996	0.996	0.985	198.1	0.01	0.0020	0.982	0.982
							−6.94	0.012		0.996				0.01	0.0009	0.982	

It is impossible to have 440, 531 and 551 reflections for the Bragg case for a plane MgO crystal cut along [100], [010] and [001] with Cu $K\alpha$ incidence, but the corresponding 'intensity' appears in Lawrence's (1973*b*) table, while in the same table the allowed Bragg-case reflections for 644, 662, 840, 842, 664, 860, 751, 911 and 753 are missing.

traditional crystallography, in particular for the case of long-wavelength X-ray diffraction and also for the case where absorption has to be considered and the low-angle information is important, as in neutron diffractometry for a magnetic structure study of rare-earth compounds. The present method also offers other possibilities, such as the evaluation of the mosaic spread of a crystal by measuring the IRPR rather than relying on angular measurement and the direct evaluation of the value of μ for neutron diffraction when the inelastic scattering effect is included.

The applicability of this theory, obviously, is for crystals with small mosaic blocks and large mosaic spread. For the other extreme case, *i.e.* a perfect plate

crystal where coherent diffraction dominates, one can gave an adequate treatment of its primary extinction. The problem, however, is how far this theory can be extended. The two conceptual difficulties involved in crystals with relatively large mosaic blocks and small mosaic spread have been pointed out by Werner (1974). Kato (1976, 1980) and Kawamura & Kato (1983) suggested that the H–D equations hold as far as $\tau_2 \leq \Lambda$, where Λ is the extinction distance and τ_2 is the correlation length of the phase factor; his criterion, in fact, is a minimum allowable η when the wavelength and reflection plane are defined. Becker (1977) suggested that the H–D equations with $\Sigma_s Y_p$ instead of Σ_s should be valid as far as $\bar{l} \leq \Lambda$, where $\bar{l}$ is the mean size of the mosaic blocks. Keeping this criterion in mind, one can see from analysis of the MgO experiment that the fitting parameter of block radius $r = 38\,\mu\text{m}$ already exceeds the Λ value of 7.3×10^{-6} m for the 200 reflection, *i.e.*, by Becker's criterion, the primary extinction is too large for the $\Sigma_s Y_p$ treatment. However, the other parameter $\eta = 0.2'$, corresponding to a τ_2/Λ value of 0.1, is within the range of applicability for the H–D equations set by Kato; the mosaic spread 28.3″, evaluated from the fitting value η, is much larger than 3.85″, the value of the Darwin width of the 200 reflection. The relatively good agreement with experimental values of extinction factors for MgO suggests that the criterion set by Becker may be too strict. All these, however, are tentative and a final judgement may require further verification and should include comparison with carefully prepared experiments carried out using several different wavelengths.

Through refinement of the data for LiF, we believe that secondary extinction may still dominate for a particular reflection at very low Bragg angle provided that (i) the size of the mosaic blocks is much less than Λ for that angle, and (ii) $\tau_2 < \Lambda$.

This method is adequate for a plane crystal in the asymmetric case. However, for an extremely asymmetric Bragg case when the angle of grazing emergence is of the order of a few minutes, *i.e.* $b < -150$, the non-applicability of the H–D equations (Sears, 1996) should be considered.

Anisotropic extinction resulting from anisotropy in a mosaic structure can also be included in the formal theory by allowing η and l in $\Sigma_s Y_p$ to depend on the Miller indices of the reflection (*ITCr*, 1995).

I am grateful to Professor T. M. Sabine of the Lucas Heights Research Laboratory, Australia, for valuable discussions. I am also grateful to Profesor E. Fawcett of the University of Toronto, Canada, Professor B. M. Craven of the University of Pittsburgh, USA, and Professor Z. Yang of the Neutron Scattering Laboratory of CIAE, China, for help and valuable suggestions about presentation.

References

Becker, P. J. (1977). *Acta Cryst.* A**33**, 243–249.
Becker, P. J. & Coppens, P. (1974). *Acta Cryst.* A**30**, 129–147, 148–153.
Borie, B. (1982). *Acta Cryst.* A**38**, 248–252.
Darwin, C. G. (1914). *Philos. Mag.* **27**, 315, 675.
Darwin, C. G. (1922). *Philos. Mag.* **43**, 800–829.
Hamilton, W. C. (1957). *Acta Cryst.* **10**, 629–634.
Hamilton, W. C. (1963). *Acta Cryst.* **16**, 609–611.
Hu, H.-C. (1997). *Acta Cryst.* A**53**, 484–492.
International Tables for X-ray Crystallography (1972). Vol. II, pp. 296–299. Birmingham: Kynoch Press.
International Tables for X-ray Crystallography (1974). Vol. III, p. 99. Birmingham: Kynoch Press.
International Tables for Crystallography (1995). Vol. C, pp. 521–524, 530–533. Dordrecht: Kluwer.
Kampermann, S. P., Sabine, T. M. & Craven, B. M. (1995). *Acta Cryst.* A**51**, 489–497.
Kato, N. (1976). *Acta Cryst.* A**32**, 453–457, 458–466.
Kato, N. (1980). *Acta Cryst.* A**36**, 171–177, 763–769, 770–778.
Kawamura, & Kato, N. (1983). *Acta Cryst.* A**39**, 305–310.
Killean, R. C., Lawrence, J. L. & Sharma, V. C. (1972). *Acta Cryst.* A**28**, 405–407.
Lawrence, J. L. (1972). *Acta Cryst.* A**28**, 400–404.
Lawrence, J. L. (1973*a*). *Acta Cryst.* A**29**, 94–95.
Lawrence, J. L. (1973*b*). *Acta Cryst.* A**29**, 208–210.
Mazzone, G. (1981). *Acta Cryst.* A**37**, 391–397.
Palmer, A. & Jauch, W. (1995). *Acta Cryst.* A**51**, 662–667.
Rigoult, J. & Guidi-Morosini, C. (1980). *Acta Cryst.* A**36**, 149–151.
Sabine, T. M. (1988). *Acta Cryst.* A**44**, 368–373.
Sabine, T. M. (1995). *International Tables for Crystallography*, Vol. C, pp. 530–533. Dordrecht: Kluwer.
Schneider, J. R. (1977). *Acta Cryst.* A**33**, 235–243.
Sears, V. F. (1996). Private communication.
Suortti, P. (1982). *Acta Cryst.* A**38**, 642–647.
Werner, S. A. (1974). *J. Appl. Phys.* **45**, 3246–3254.
Wilkins, S. W. (1981). *Proc. Philos. Trans.* **299**, 275–317.
Yelon, W. B., van Laar, B., Kaprzyk, S. & Maniawski, F. (1984). *Acta Cryst.* A**40**, 16–23.
Yelon, W. B., van Laar, B., Maniawski, F. & Kaprzyk, S. (1984). *Acta Cryst.* A**40**, 24–31.
Zachariasen, W. H. (1967). *Acta Cryst.* **23**, 558–564.
Zachariasen, W. H. (1968). *Acta Cryst.* A**24**, 324–325.